2015

Overaccumulation of γ-Glutamylcysteine in a Jasmonate-Hypersensitive Arabidopsis Mutant Causes Jasmonate-Dependent Growth Inhibition

Hsin-Ho Wei
University of Nebraska-Lincoln

Martha Rowe
University of Nebraska-Lincoln

Jean-Jack M. Riethoven
University of Nebraska-Lincoln, jeanjack@unl.edu

Ryan Grove
University of Nebraska-Lincoln

Jiri Adamec
University of Nebraska-Lincoln, jadamec2@unl.edu

See next page for additional authors

Overaccumulation of γ-Glutamylcysteine in a Jasmonate-Hypersensitive Arabidopsis Mutant Causes Jasmonate-Dependent Growth Inhibition[1][OPEN]

Hsin-Ho Wei, Martha Rowe, Jean-Jack M. Riethoven, Ryan Grove, Jiri Adamec, Yusuke Jikumaru, and Paul Staswick*

Department of Agronomy and Horticulture, University of Nebraska, Lincoln, Nebraska 68583 (H.-H.W., M.R., P.S.); Center for Biotechnology (J.-J.M.R.), and Department of Biochemistry (R.G., J.A.), University of Nebraska, Lincoln, Nebraska 68588; and Riken Plant Science Center, Yokohama 230–0045, Japan (Y.J.)

ORCID IDs: 0000-0002-2709-7880 (J.-J.M.R.); 0000-0002-8810-6509 (Y.J.); 0000-0003-2798-0275 (P.S.).

Glutathione (GSH) is essential for many aspects of plant biology and is associated with jasmonate signaling in stress responses. We characterized an Arabidopsis (*Arabidopsis thaliana*) jasmonate-hypersensitive mutant (*jah2*) with seedling root growth 100-fold more sensitive to inhibition by the hormone jasmonyl-isoleucine than the wild type. Genetic mapping and genome sequencing determined that the mutation is in intron 6 of *GLUTATHIONE SYNTHETASE2*, encoding the enzyme that converts γ-glutamylcysteine (γ-EC) to GSH. The level of GSH in *jah2* was 71% of the wild type, while the *phytoalexin-deficient2-1* (*pad2-1*) mutant, defective in *GSH1* and having only 27% of wild-type GSH level, was not jasmonate hypersensitive. Growth defects for *jah2*, but not *pad2*, were also seen in plants grown to maturity. Surprisingly, all phenotypes in the *jah2 pad2-1* double mutant were weaker than in *jah2*. Quantification of γ-EC indicated these defects result from hyperaccumulation of this GSH precursor by 294- and 65-fold in *jah2* and the double mutant, respectively. γ-EC reportedly partially substitutes for loss of GSH, but growth inhibition seen here was likely not due to an excess of total glutathione plus γ-EC because their sum in *jah2 pad2-1* was only 16% greater than in the wild type. Further, the *jah2* phenotypes were lost in a jasmonic acid biosynthesis mutant background, indicating the effect of γ-EC is mediated through jasmonate signaling and not as a direct result of perturbed redox status.

Glutathione (GSH) is an essential thiol of most higher organisms, including plants. Primarily found in the reduced form, its roles in maintaining a reduced intracellular state are numerous and well characterized (Foyer and Noctor, 2011; Noctor et al., 2011). Additionally, GSH is involved in detoxifying reactive oxygen species, heavy metal detoxification through phytochelatins, elimination of xenobiotics, and signaling of plant development and stress responses (Rouhier et al., 2008).

GSH is synthesized in two steps. The first links Cys to the γ-carboxyl group of Glu through an amide bond catalyzed by γ-glutamylcysteine (γ-EC) synthetase, encoded by the single gene *GSH1* in Arabidopsis (*Arabidopsis thaliana*). Gly is then added by GSH synthetase (GSH-S), also encoded by a single gene (*GSH2*). GSH is typically present at millimolar levels in plants, and although γ-EC is normally present at only a few percent of this amount, there is evidence that γ-EC has redox activities in Arabidopsis (Pasternak et al., 2008).

Insertional knockouts of *GSH1* are embryo lethal, and *rootmeristemless1*, with only 5% of wild-type GSH level, lacks a root apical meristem due to cell cycle arrest (Vernoux et al., 2000; Cairns et al., 2006). Other mutants producing 25% to 50% of wild-type GSH levels grow normally but exhibit defects under various stress conditions. For example, *phytoalexin-deficient2-1* (*pad2-1*) and *cadmium sensitive2* mutants are susceptible to pathogens and hypersensitive to Cd, respectively, while *regulator of axillary meristems1* causes elevated expression of *ASCORBATE PEROXIDASE2* under non-photooxidative-stress conditions (Glazebrook and Ausubel, 1994; Cobbett et al., 1998; Ball et al., 2004).

GSH2 null alleles (*gsh2-1* and *gsh2-2*) are also lethal, although plants survive to the early seedling stage (Pasternak et al., 2008). Survival past the embryo stage was attributed to partial complementation of GSH activity by γ-EC, which accumulates to excessive levels in *gsh2-1*, and the mutant is partially rescued by GSH supplementation. Missense and nonsense *GSH2* alleles of membrane trafficking mutants (*gsh2-3*–*gsh2-5*) disrupt

[1] This work was supported in part by the U.S. Department of Agriculture National Institute of Food and Agriculture (Hatch project no. NEB–22–357), the National Science Foundation (grant no. IOS–0744758 to P.S.), and the Nebraska Research Initiative (to J.-J.M.R.).

* Address correspondence to pstaswick1@unl.edu.

The author responsible for distribution of materials integral to the findings presented in this article in accordance with the policy described in the Instructions for Authors (www.plantphysiol.org) is: Paul Staswick (pstaswick1@unl.edu).

H.-H.W. did gene mapping and mutant hormone response experiments, J.-J.M.R. analyzed whole-genome sequencing data, R.G. and J.A. quantified glutathione by liquid chromatography/mass spectrometry, Y.J. developed jasmonate response gene primers, and P.S. and M.R. did all other experiments.

[OPEN] Articles can be viewed without a subscription.
www.plantphysiol.org/cgi/doi/10.1104/pp.15.00999

endoplasmic reticulum (ER) organization and also arrest growth in early seedling development, while a weaker allele (*gsh2-6*) reached maturity but was smaller than the wild type (Au et al., 2012). A screen for reduced response to Cd also yielded a viable missense mutant of *GSH2* (*nonresponse or reduced response to Cd2*) with approximately 75% of the wild-type GSH level (Jobe et al., 2012).

Plant oxidative stress responses involve both redox signaling through GSH and jasmonate hormonal signaling, and gene expression studies have clearly linked these two signaling systems. GSH biosynthesis and metabolism genes are induced by jasmonate, while manipulating GSH level or redox status in various mutants alters expression of genes for jasmonate biosynthesis and signaling (Xiang and Oliver, 1998; Mhamdi et al., 2010; Han et al., 2013). GSH and jasmonate are also associated with protective glucosinolate production in response to insect feeding (Noctor et al., 2011). For example, *pad2-1* is deficient in glucosinolates and more susceptible to insects, while several studies have shown jasmonate induces glucosinolates (Brader et al., 2001; Mikkelsen et al., 2003; Sasaki-Sekimoto et al., 2005; Schlaeppi et al., 2008). Liu et al. (2010) isolated *jasmonic acid hypersensitive1* (*jah1*), an Arabidopsis mutant with greater inhibition of root growth than the wild type in the presence of jasmonic acid (JA). The affected gene encodes a cytochrome P450 (CYP82C3) involved in indole glucosinolate production, and this mutant was more susceptible to *Botrytis cinerea*.

The basic mechanism of jasmonate signal transduction and some of the downstream responses emanating from it are now well understood (Browse, 2009; Wasternack and Hause, 2013). However, the mechanisms by which jasmonate and GSH coordinate their activities to mediate oxidative stress and other responses are not known. This study characterized, to our knowledge, a new jasmonate-hypersensitive mutant that accumulates excess γ-EC due to a defect in *GSH2*, but GSH is only modestly reduced. Results show that elevated γ-EC is deleterious to plant growth through a jasmonate-dependent mechanism.

RESULTS

Characterization of a New Jasmonate-Hypersensitive Mutant

Screening of Arabidopsis seedlings from an ethyl methanesulfonate mutagenized population (Columbia [Col-0] ecotype) in the presence of the auxin inhibitor JA-Trp yielded a mutant that was markedly suppressed in root growth compared with the wild type (Staswick, 2009). Further analysis showed the phenotype was not due to JA-Trp directly but rather to small amounts of JA, apparently either a minor contaminant in the JA-Trp preparation or produced by conjugate hydrolysis after JA-Trp assimilation. This mutant has been called *jah2* (Wei, 2012). Figure 1A shows that 50% inhibition of root growth for *jah2* occurred at approximately 50 nM for both the active hormone JA-Ile and jasmonic acid methylester (MeJA), the latter being metabolized to JA-Ile in planta. The concentration necessary for similar inhibition of wild-type roots was approximately 100-fold higher. Shorter roots in the absence of jasmonate were also consistently seen for *jah2*: 21.7 mm (SE = 0.8) for the wild type and 16.4 mm (SE = 0.5) for *jah2* in the experiment described here (ANOVA, $P = 1.22 \times 10^{-6}$, $n = 18$).

To assess whether response to other hormones was affected in *jah2*, root growth was determined in the presence of inhibiting concentrations of indole-3-acetic acid (IAA) or the ethylene precursor ACC. We found no evidence that *jah2* root growth on IAA was affected differently than for the wild type (Fig. 1B). Growth on aminocyclopropane-1-carboxylic acid (ACC) was actually greater for *jah2* than the wild type, although the concentration for 50% inhibition was only about 2-fold higher.

To test whether the hyperresponse to jasmonate was dependent on the CORONATINE INSENSITIVE1 (COI1) jasmonate receptor-signaling pathway, we evaluated *jah2* root growth in a *coi1* mutant background. On medium lacking added MeJA, *jah2 coi1* was restored to wild-type root length (Fig. 1C). On 0.5 μM MeJA, the double mutant *jah2 coi1* was also not significantly different from the wild type, while *jah2* seedlings heterozygous for the recessive *coi1* mutation were only slightly longer than *jah2* (Fig. 1D). Thus, the short-root phenotype of *jah2* is largely dependent on the jasmonate-signaling pathway involving JA-Ile and COI1.

The jasmonate content of fully expanded *jah2* leaves was determined to assess whether differences in synthesis or metabolism of jasmonates might explain the hypersensitivity (Suza and Staswick, 2008). The basal level of JA was 39.8 (SE = 10.2) and 29.7 (SE = 3.7) pmol g^{-1} fresh weight (FW) for the wild type and *jah2*, respectively, but these were not significantly different (ANOVA, $P = 0.399$, $n = 3$ biological replicates). The basal level of the jasmonate signal, JA-Ile, was undetectable in both genotypes. JA and JA-Ile at 0.5, 1, 2.5, and 6 h following leaf wounding also showed essentially the same kinetics and quantity of accumulation in the wild type and *jah2* (data not shown) as seen previously (Suza and Staswick, 2008). These results suggest that hypersensitivity in *jah2* is not due to a differential ability to accumulate or metabolize JA or JA-Ile compared with the wild type.

jah2 Is Defective in *GLUTATHIONE SYNTHETASE2*

Figure 2A summarizes results from genomic mapping with PCR-based markers that placed the *JAH2* locus on chromosome 5 between nucleotides 9,598,367 and 9,775,141, an interval containing at least 60 putative open reading frames. Thus, *jah2* defines a different locus than *jah1* (At4g31970), which is located on chromosome 4. We next used whole-genome sequencing to search for single nucleotide polymorphisms (SNPs) compared with the wild type, possibly caused by ethyl methanesulfonate mutagenesis. The *jah2* sequence data were aligned with the wild-type Col-0 reference genome

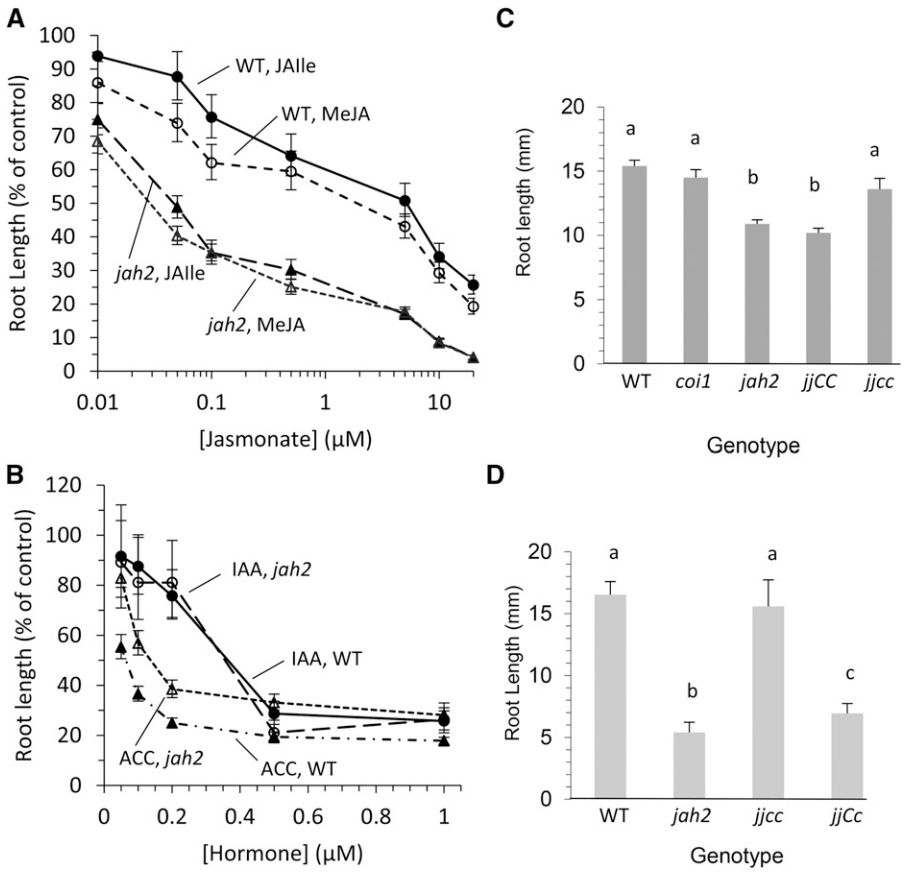

Figure 1. Characterization of *jah2*. A, Primary root growth of the wild type (WT) and *jah2* on agar plates in the presence of JA-Ile or MeJA. Length was measured after 5 d of growth, and values are means of 18 seedlings, expressed as percentage of length for each genotype in the absence of jasmonate. Error bars are 95% confidence intervals. B, Same as A for growth on IAA or the ethylene precursor ACC ($n = 20$ seedlings). C, Growth of *jah2* roots in the *coi1* jasmonate coreceptor mutant background. Seeds from a *jah2* homozygous plant segregating for *coi1* were grown on the surface of vertical agar plates on control medium. Five-day-old seedlings were measured and genotyped for *COI1*. *jj* indicates homozygous for *jah2*; *cc* indicates homozygous for *coi1* mutant; and *CC* and *Cc* indicate the wild type and heterozygous (wild phenotype) for *COI1*, respectively. Error bars show SE, and means significantly different are denoted with different letters (ANOVA, $P \leq 0.01$, $n = 10$ seedlings). D, As in C, except growth was 6 d on 0.5 μM MeJA ($n = 15$).

(see "Materials and Methods" and Supplemental Table S1). Within the mapped interval, only two strong candidates for polymorphisms were found: G-to-A transitions at positions 9,669,462 and 9,747,219. The latter is in an intergenic region, while the first is in intron 6 of *GSH2* (Fig. 2A).

The polymorphism in *GSH2* creates an *Ssp*I restriction endonuclease site that was used to develop a genomic cleaved amplified polymorphic sequence (CAPS) marker using the PCR primer sites shown (Fig. 2A). Analysis by PCR confirmed the nucleotide change in *jah2* (data not shown). GSH2 intron 6 is unusual in that it contains AT-AC ends rather than the typical GT-AG ends. These rare introns are excised via the U12 spliceosome, rather than the U2 complex used for most introns (Sharp and Burge, 1997; Lewandowska et al., 2004). A distinguishing feature of U12-spliced introns is a highly conserved ATATCCT sequence at their 5′ end. The polymorphism in the *jah2* allele occurs at the fifth nucleotide of this sequence, a C-to-T transition, suggesting it might affect processing or stability of the *GSH2* transcript. Northern-blot hybridization was used to compare *GSH2* transcripts from leaves of the wild type and *jah2*. *GSH2* is up-regulated by jasmonate, but both the basal and induced transcript levels were markedly lower in *jah2* compared with the wild type (Fig. 2B). Further, the major transcript in the mutant was larger, possibly the result of defective splicing. To test this hypothesis, we analyzed complementary DNA (cDNA) by PCR with the primers noted above. The expected product size for the wild type is 297 bp, consistent with what is seen in Figure 2C. *jah2* also produced a minor product of this size, but the majority of DNA was about 100 bp larger. This is consistent with the retention in the cDNA of intron 6, which is 108 bp. Digestion of the samples with *Ssp*I confirmed the presence of this restriction site only in the larger fragment from *jah2* but not in the smaller fragment from the wild type or *jah2* (Fig. 2C). Together, this evidence suggests that a substantial portion of the *jah2 GSH2* mRNA retains intron 6, although a minor amount appears to be correctly processed at this site.

To examine whether a defective *GSH2* is responsible for the root phenotype of *jah2*, we transformed the mutant with a wild-type *GSH2* cDNA regulated by the *Cauliflower mosaic virus* 35S promoter. Analysis of cDNA by PCR (Fig. 2D) shows that in addition to the upper intron-containing PCR product, two independently transformed lines (*jah2*:*GSH4-3* and *jah2*:*GSH16-3*) contain a much stronger band, consistent with the wild-type PCR product, indicating the wild-type transgene is effectively expressed. Figure 3A shows that root growth of the complemented *jah2* lines on MeJA was clearly greater than for *jah2*, nearly or completely restoring it to wild-type growth, depending on MeJA concentration.

GSH synthetase enzyme activity was also examined. Activity in *jah2* was only approximately 10% of the wild

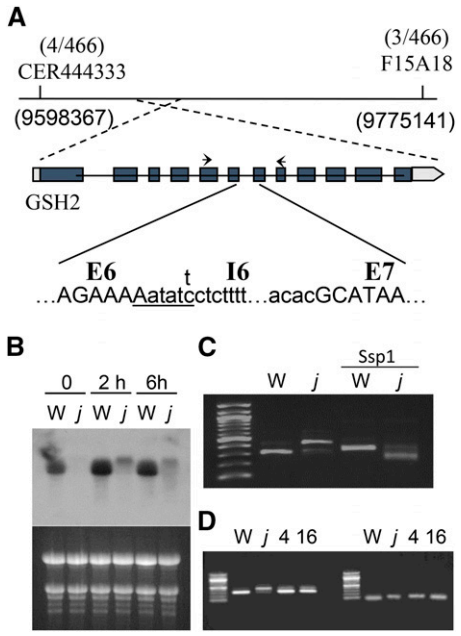

Figure 2. Identification of the *jah2* mutation. A, The locus mapped between CAPS markers indicated on chromosome 2; number of recombinant chromosomes in 466 F2 individuals shown at top. Genome sequence analysis found an SNP in intron 6 of *GSH2* (At5G27380.1). Reference genome sense strand for *GSH2* surrounding the SNP is shown at the bottom, with t above the sequence indicating the C-to-T transition in *jah2*. Underlined nucleotides denote the *Ssp*I restriction site created in *jah2*. Short arrows above exons 5 and 8 indicate primer sites for PCR analysis. B, Northern-blot hybridization of RNA from wild-type (W) and *jah2* (*j*) seedlings grown 6 d in liquid medium followed by 0-, 2-, or 6-h incubation in 10 μM MeJA. Hybridization was with a full-length *GSH2* cDNA probe. Bottom section shows total RNA from the original gel stained with ethidium bromide. C, PCR of cDNA over the interval flanked by primer sites in A. To the right are the same samples digested with *Ssp*I. Molecular weight markers at the left are at 100-bp intervals, starting with 100 bp at the bottom. D, PCR analysis of cDNA from two transformed *jah2* lines complemented with the full-length wild-type *GSH2* cDNA, *jah2*:*GSH4-3* (4), and *jah2*:*GSH16-3* (16). To the right are the same cDNA samples amplified with *ACTIN8* primers as a control.

type, while for the two transformants, activity was restored to essentially the same as wild-type level (Fig. 3B). This evidence further suggests that the phenotype in *jah2* is due to a loss of *GSH2* function. To explore whether a GSH deficiency could be the cause of root jasmonate hypersensitivity, we attempted to complement the phenotype with exogenous GSH. In the absence of MeJA, GSH at 0.5 mM restored *jah2* mutant roots to wild-type length (Fig. 3C). In the presence of 0.5 μM MeJA, 1 mM GSH complemented the mutant to wild-type growth. In both cases, GSH had little or no inhibitory effect until concentrations were above 1 mM.

The *jah2* Phenotype Is Not Due to GSH Deficiency

Although complementation with exogenous GSH suggested the defect in *jah2* might be a deficiency of GSH, the value determined by gas chromatography (GC)/mass spectrometry (MS) for total glutathione in *jah2* was only about 30% less than in the wild type (Table I). Accuracy of this assay was enhanced by the synthesis of stable isotopes of GSH and γ-EC for use as internal standards. GSH was also determined by an independent liquid chromatography (LC)/MS method that distinguished between reduced and oxidized GSH (GSSG). This method also found the quantity of both

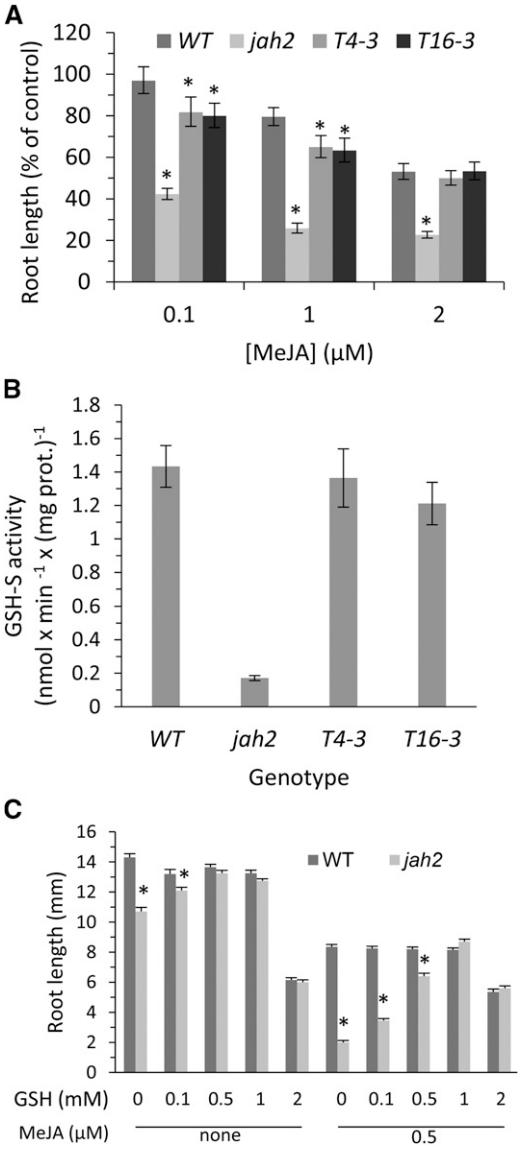

Figure 3. Mutant characterization. A, Complementation of the *jah2* root phenotype with a *GSH2* cDNA transgene. *T4-3* and *T16-3* are the transformants described in Figure 2. Seedling roots after 5 d growth on MeJA. Errors are 95% confidence intervals (n = 20). Asterisks indicate significant difference from the wild type (WT) within treatments (ANOVA, $P \leq 0.05$). B, GSH2 enzyme activity in leaves. Prot., Protein. C, Seedling root growth with exogenous GSH. Measurements were after 6 d of growth with supplementations at initial concentrations as indicated. Error bars are SE (n = 20 seedlings). Asterisks indicate *jah2* significantly different from the wild type within treatments (ANOVA, $P \leq 0.01$).

were only modestly lower in *jah2* than in the wild type (Supplemental Fig. S1). As expected, in these unstressed plants, the amount of GSSG was approximately 10% of total glutathione for all genotypes (Noctor et al., 2011). The *pad2-1* mutant that affects *GSH1* had only about 25% of the wild-type level of total glutathione (Table I; Supplemental Fig. S1), consistent with published results, and the double mutant *jah2 pad2-1* contained somewhat less GSH than *pad2-1* (Parisy et al., 2007).

The much lower levels of GSH in *pad2-1* and the double mutant than in *jah2* prompted us to investigate their root response to MeJA. Surprisingly, *pad2-1* was no more sensitive than the wild type when grown on 1 and 5 μM MeJA (Fig. 4A). Furthermore, the double mutant was less hypersensitive than *jah2*, even though it contained the least amount of GSH.

The discrepancy between phenotype and GSH levels among these mutants showed that GSH deficiency was not the cause of the hyperresponse in *jah2*. An alternate hypothesis is that *jah2* overaccumulates the biosynthetic intermediate γ-EC due to insufficient GSH-S enzyme activity. Consistent with this, *jah2* accumulated γ-EC to 1,764 nmol g^{-1} FW, which is 294-fold higher than in the wild type, but still only 4.5 times the level of GSH in the wild type (Table I). Of the total γ-EC in *jah2*, 32.9% (SE = 3.1, $n = 4$) was in the oxidized form (data not shown). The double mutant had 394 nmol g^{-1} FW of γ-EC, approximately 66-fold higher than in the wild type, but essentially the same level as GSH in the wild type. In the *jah2* lines complemented for *GSH2* by transformation, γ-EC was reduced to near wild-type level (Table I).

We next determined whether exogenous γ-EC inhibited seedling root growth. In the absence of MeJA, 0.2 mM γ-EC resulted in 87% and 82% of the growth on control medium for the wild type and *pad2-1*, respectively (Fig. 4B, bar 1 for each genotype). By contrast, growth of *jah2* was not significantly reduced by γ-EC in the absence of exogenous MeJA (100% of control), while only a 5% reduction occurred in the double mutant. In the presence of MeJA at 0.2 and 1 μM, γ-EC further inhibited growth in the wild type and *pad2-1* (bars 2 versus 3 and 4 versus 5 for each genotype). By contrast, γ-EC did not further reduce growth on MeJA for *jah2* or *jah2 pad2-1*, possibly because endogenous γ-EC levels were already sufficiently high to have the maximum inhibitory effect. Altogether, the results support the hypothesis that excess accumulation of γ-EC, not a deficiency in GSH, leads to jasmonate-hypersensitive root growth.

The role of excess γ-EC in hypersensitivity is at odds with the fact that exogenous GSH complements the root phenotype of *jah2* (Fig. 3C). One possible explanation is that GSH reduces γ-EC accumulation by feedback inhibition of GSH-S enzyme activity (Hell and Bergmann, 1990). The level of γ-EC in *jah2* seedling roots was more than twice that determined for aerial tissue (Table I). Growth for 6 d on agar plates containing 1 mM GSH reduced this level by nearly 75%. However, γ-EC was still greatly above that in the wild-type control, suggesting that feedback inhibition may not be the only mechanism by which GSH restores root growth in *jah2*.

Table I. *Quantitation of thiols by GC/MS*

Values are means of three replicates (SE). Values with same letter for each thiol for aerial tissue are not significantly different (ANOVA, $P < 0.05$). nd, Not determined.

Sample	GSH	γ-EC
	nmol × g^{-1} FW	
Aerial tissue		
Wild type	395.6 (14.2)[a]	6.0 (0.5)[a]
jah2	281.1 (15.0)[b]	1,764.0 (172.2)[b]
pad2	109.2 (7.0)[c]	3.3 (0.1)[c]
jah2 pad2	72.2 (6.8)[c]	393.5 (44.8)[d]
jah2:GSH4-3	278.9 (38.2)[b]	15.0 (1.4)[e]
jah2:GSH16-3	348.9 (35.5)[a,b]	9.8 (0.7)[a,e]
dde2 jah2	238.8 (31.8)[b]	1,209.0 (60.8)[f]
Seedling roots		
Wild-type control	nd	6.9 (0.8)
jah2 control	nd	4,118.7 (210.9)
jah2 plus GSH	nd	1,180.4 (157.5)

jah2 Plants Are Compromised in Growth in Soil

Growth of *jah2* plants in soil consistently resulted in smaller rosettes, fewer leaves, and earlier flowering than the wild type. Representative plants at 16 d after seed sowing are shown in Figure 5A. Pasteurized soil and a clean growth incubator were used to limit possible effects of pests or pathogens. *jah2* plants exhibited a stunted growth phenotype with shorter leaf blades and petioles. As seen for root sensitivity to MeJA, the double mutant was intermediate in phenotype between the single mutant and the wild type. Mean diameter of rosettes, measured as the greatest distance between two leaf tips at 20 d after planting, were 22.7 (SE = 1.3 mm), 31.7 (SE = 0.9 mm), and 45.6 mm (SE = 1.1 mm) for *jah2*, *jah2 pad2-1*, and the wild type, respectively. Each mean was significantly different from the other two (ANOVA, $P \leq 0.1$, $n = 19$ plants each). The growth of *pad2-1* was not different from the wild type, consistent with observations of others (Parisy et al., 2007). Similar results were found in three independent experiments. Leaf numbers on days 19, 23, and 28 followed the same trend, with significantly fewer leaves than the wild type for *jah2* and *jah2 pad2-1* on all days, except the difference was not significant on day 28 for the double mutant (Fig. 5B). The double mutant also had significantly more leaves than *jah2* on all days examined. Despite their delayed vegetative development, *jah2* plants flowered earlier than the wild type, reaching approximately 50% on day 30, while the wild type and *pad2-1* were approximately 6 d later for 50% flowering (Fig. 5C). Again, the double mutant was intermediate in flowering time. Transgenically complemented *jah2* was phenotypically the same as the wild type for all measurements shown here (data not shown).

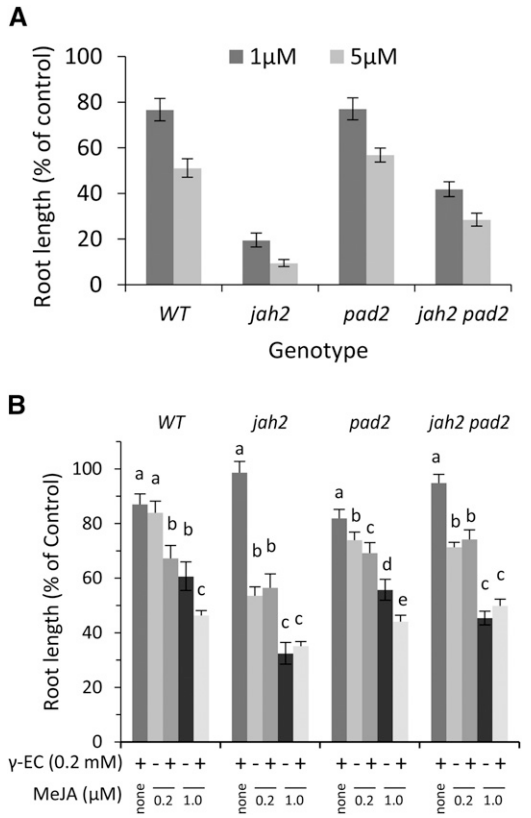

Figure 4. Mutant primary root growth. A, Growth on MeJA as described in Figure 3A. B, Root growth on MeJA and γ-EC at indicated initial concentrations. Values are percentages of growth for 6 d on control medium for each genotype, with 95% confidence intervals shown (n = 25 seedlings). Within genotypes, means with same letter are not significantly different (ANOVA, $P \leq 0.01$). WT, Wild type.

Growth Inhibition Is Jasmonate Dependent

To assess whether these growth defects are jasmonate dependent, we combined *jah2* with the *delayed dehiscence2-2* (*dde2-2*) allele, which is a mutation in the *ALLENE OXIDE SYNTHASE* gene, leading to essentially no JA accumulation (von Malek et al., 2002). Growth of this double mutant was restored to essentially the same as the wild type and the *dde2-2* mutant alone (Fig. 5D). Leaf number for the double mutant was also not different from the wild type, and flowering time was only slightly earlier than the wild type, but clearly later than *jah2* (Fig. 5, E and F). As expected, seedling root growth in the double mutant exhibited the same sensitivity to jasmonate as for *jah2*, when MeJA was supplied exogenously (Fig. 5G). We also examined whether the γ-EC content of *jah2 dde2-2* was altered compared with *jah2*. γ-EC in *jah2 dde2-1* was reduced by approximately 30% compared with *jah2*, while GSH was not significantly different from *jah2*. Therefore, restored growth in the double mutant was not due to a marked decline in γ-EC, confirming that endogenous jasmonate is the primary factor inhibiting growth in *jah2*.

Several Jasmonate-Responsive Genes Are Not Hypersensitive to Jasmonate in *jah2*

To assess whether jasmonate-dependent gene expression is also hypersensitive in *jah2*, we examined induction of several genes by MeJA in 7-d-old seedlings grown in sterile liquid culture. A relatively low concentration of MeJA (2 μM) and early induction time points were examined to maximize the opportunity to detect a hyperresponse. Well-characterized representative genes for JA biosynthesis (*OXOPHYTODIENOATE REDUCTASE3* and *LIPOXYGENASE2*), jasmonate signaling (*JASMONATE ZIM DOMAIN1* [*JAZ1*], *JAZ9*, and *JAZ10*), and defense response (*PLANT DEFENSIN1.2* [*PDF1.2*] and *THIONIN2.1* [*THI2.1*]) and *VEGETATIVE STORAGE PROTEIN1* (*VSP1*) and *VSP2* were analyzed by semiquantitative PCR or northern-blot hybridization. For these experiments, seedlings for each time point and genotype originated from separate cultures. Figure 6 shows that all gene transcripts were elevated in response to MeJA, but there was no evidence for a hyperresponse in *jah2* relative to the wild type, either in degree or timing of induction. In fact, *PDF1.2* transcript was lower in the mutant after 12 and 24 h, although not different from the wild type up to 6 h. Transcripts for *VSP2* and *JAZ10* were also modestly lower in *jah2* at several time points. Whatever the mechanism of root hypersensitivity to exogenous MeJA, it does not extend generally to hypersensitive induction of the genes examined here.

DISCUSSION

A major advance in this study is that we have clearly separated effects of excess γ-EC from those of GSH deficiency in relation to plant growth and jasmonate response. The leaky mutation in *jah2* permits hyperaccumulation of γ-EC, with minimal effect on the amount of GSH. Null *GSH2* alleles vastly overaccumulate γ-EC but are lethal. Previously described leaky alleles accumulating several times more γ-EC than *jah2* (e.g. *gsh2-1–gsh2-6*) also are more deficient in GSH, making interpretation of their phenotypes less clear. In fact, growth deficiency in these mutants has previously been attributed to insufficient GSH, which the excess γ-EC incompletely compensates for (Pasternak et al., 2008; Au et al., 2012). By contrast, our results indicate that an excess of γ-EC with near normal levels of GSH inhibits growth, while similar defects were not found in *pad2-1*, which has much less GSH and near normal γ-EC level. Further, phenotypes were less severe in the double mutant *jah2 pad2-1*, apparently due to its decreased γ-EC accumulation compared with *jah2*. The sum of GSH and γ-EC was only slightly higher in the symptomatic double mutant than in the wild type, suggesting it is not an excess of total thiols that is detrimental.

The level of γ-EC in wild-type plants is typically only a few percent of the GSH (Cairns et al., 2006; Pasternak et al., 2008; Au et al., 2012). Our results clearly demonstrate that γ-EC has unique activities compared with

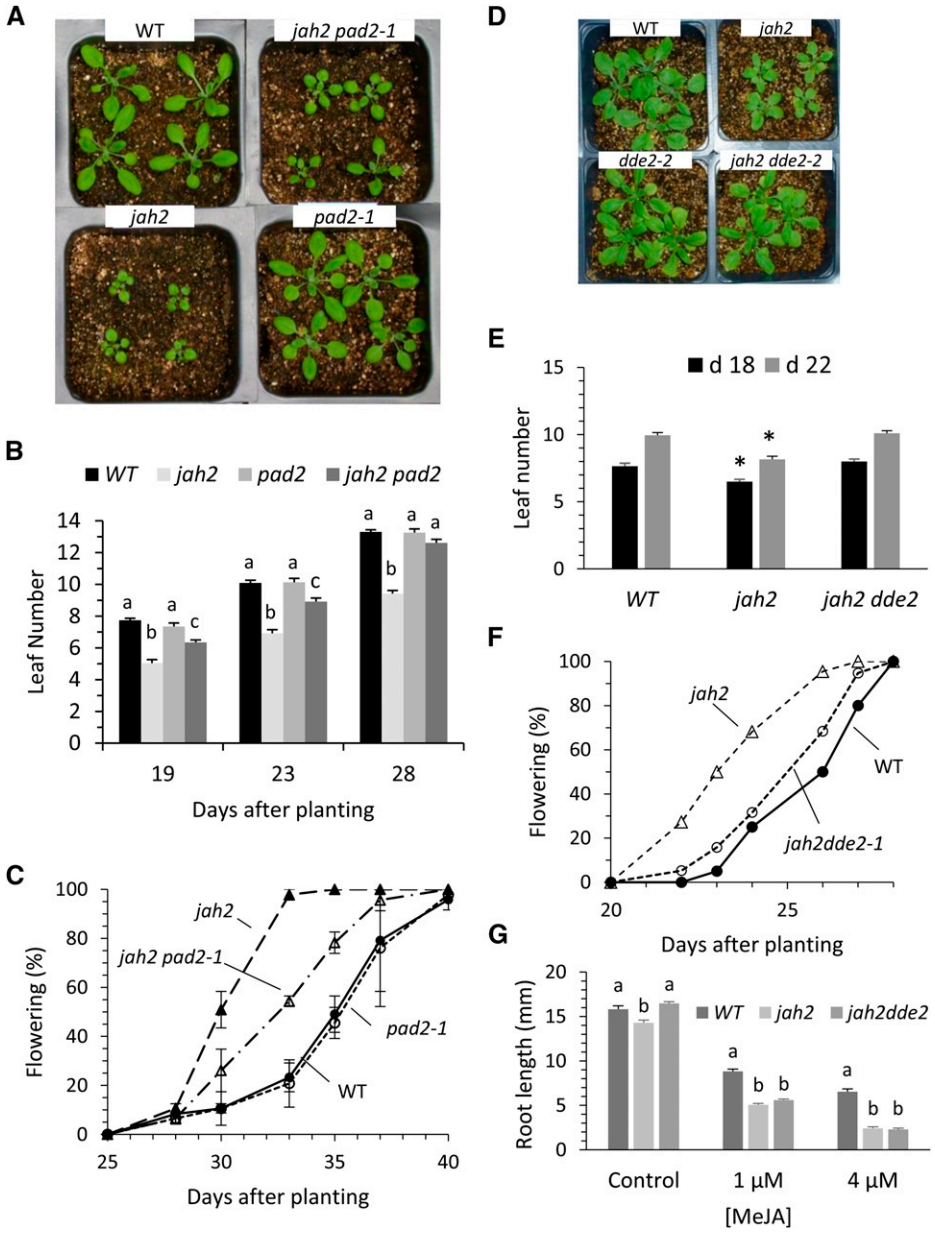

Figure 5. Growth of mutants in soil. A, Image at 16 d after planting, 11-h-light/13-h-dark photoperiod. B, Number of leaves in A at least 1 mm across on days indicated. Values are means with SE (n = 23 plants). Means with same letter are not significantly different between genotypes on the indicated day after planting (ANOVA, $P \leq 0.01$). C, Mean number of days to flower for plants in A and in a second independent experiment. Bars show SE (n = 23 plants). D, Growth of *jah2* in the *dde2* JA-deficient background at 20 d of growth, 12-h/12-h photoperiod. E, Same measurement as for B for plants described in D. Asterisks indicate significant difference from the wild type (WT) on indicated day (ANOVA, $P \leq 0.01$). F, Number of days to flower (n = 20 plants). G, Mean root length (7 d) with SE (n = 17). Means with same letter are not significantly different within treatments (ANOVA, $P \leq 0.01$).

GSH, requiring its tight control in plants. This is accomplished primarily by conversion of γ-EC to GSH. Although *jah2* has only 4.5 times more γ-EC than the normal amount of GSH, and γ-EC level in *jah2 pad2-1* is equal to that of GSH in the wild type, both are compromised in growth. By contrast, GSH up to 20-fold higher than normal in transgenic tobacco (*Nicotiana tabacum*) plants expressing a bifunctional γ-EC-ligase/GSH-S had no phenotypic effect (Liedschulte et al., 2010). On the other hand, overexpression of a γ-EC-ligase in tobacco resulting in up to 25-fold elevated γ-EC yielded plants displaying pathogenesis-related necrotic lesions, although these plants also had 3 to 5 times the normal GSH level (Creissen et al., 1999). We saw no evidence of lesions in *jah2* despite having far more γ-EC than the tobacco lines, suggesting that the consequence of excess γ-EC may vary with plant species.

Supplementation of medium with GSH restored normal jasmonate sensitivity in *jah2*. Although interpretation of these results is complicated by the fact that GSH in growth medium is unstable, the nearly 4-fold decrease in root γ-EC under this condition is consistent with negative feedback inhibition on γ-EC synthetase enzyme activity (Hell and Bergmann, 1990). However, γ-EC was still almost 170-fold higher than in control wild-type roots, suggesting other mechanisms may also be involved. Exogenous GSH might provide a higher ratio of GSH to γ-EC, possibly ameliorating some of the negative effects of excess γ-EC. Seedling lethality in *gsh2* null alleles, which are devoid of GSH, is also

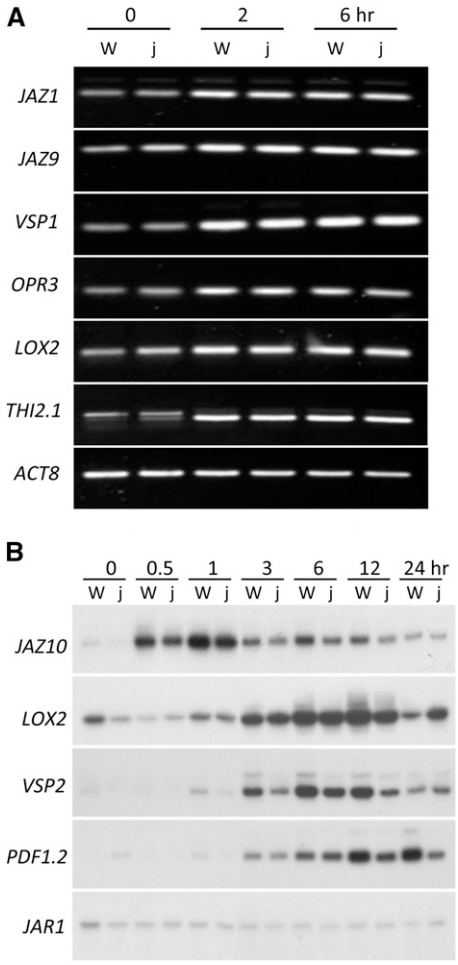

Figure 6. Induction of jasmonate response genes. Seven-day-old wild-type (w) and *jah2* (j) seedlings grown in liquid culture were treated with 2 μM MeJA and harvested for RNA extraction at the times indicated. Each time point/genotype is an independent culture. A, Semiquantitative PCR for the transcripts indicated. Primers used are shown in Supplemental Table S2. B, Northern-blot analysis with the cDNA probes indicated. The same blot was washed and reused for successive probes. *ACTIN8* (*ACT8*) and *JASMONATE RESISTANT1* (*JAR1*) are noninducible controls for A and B, respectively. *OPR, OXOPHYTODIENOATE REDUCTASE; LOX, LIPOXYGENASE.*

partially rescued by exogenous GSH. In addition to supplying necessary GSH, it is possible that the excess GSH in this case helps compensate for the high level of γ-EC as well (Pasternak et al., 2008). Au et al. (2012) characterized several secretory membrane-trafficking mutants that are viable *gsh2* alleles but more severe than *jah2*. Similar to what we found, GSH at 1 mM restored seedling root growth of *gsh2-5* to normal. This mutant accumulates about 30% of normal GSH and a little more than twice the γ-EC compared with our mutant. In addition to ER defects, growth of *gsh2-5* was strongly inhibited at the seedling stage. Partial complementation of this phenotype with GSH led the authors to conclude that a deficiency in GSH was responsible for the inhibited growth, although disruption of ER formation was attributed to the excess γ-EC (Au et al., 2012). However, the fact that *pad2-1* has similarly low GSH levels as *gsh2-5*, yet shows no seedling abnormalities, suggests that the vast excess of γ-EC is primarily responsible for the growth defects in the *gsh2-5* allele.

As already noted, the mechanism for γ-EC activity in *jah2* does not appear to result from an excess of total glutathione plus γ-EC, although we have not quantified other thiols (e.g. Cys). It is possible that γ-EC, with an active sulfhydryl, interferes with GSH by interacting with components normally targeted by GSH, but it then cannot carry out the necessary functions of GSH. Alternatively, rather than simply being an intermediate in GSH synthesis, γ-EC might have unrecognized and unique roles in redox or signaling responses that, nevertheless, require it to be in limited quantity or in the proper balance with GSH. Redox activities for γ-EC that are somewhat different, yet partially compensate for loss of GSH, have been noted in yeast (*Saccharomyces cerevisiae*) and animal cells (Grant et al., 1997; Ristoff et al., 2002; Quintana-Cabrera and Bolaños, 2013).

Only about 10% of normal GSH-S activity was detected in *jah2*, consistent with the fact that the *GSH2* transcript lacking intron 6 is only a minor fraction of the total. Despite this low enzyme level, GSH was only reduced by 30%. It seems likely that, under stress conditions that necessitate higher GSH synthesis, the deficiency in *jah2* would be greater. Pasternak et al. (2008) complemented a *gsh2* null mutant with a truncated *GSH* cDNA lacking the chloroplast transit peptide coding sequence and obtained lines having 40% to 50% of normal GSH-S activity. Their lines only modestly overaccumulated γ-EC (4- to 8-fold), consistent with the higher enzyme activity than we observed in *jah2*, and they saw no phenotypic difference from wild-type plants.

An important discovery from this study is that the *jah2* phenotype is jasmonate dependent and apparently not a direct consequence of insufficient redox activity. The essentially complete absence of jasmonate in *jah2 dde2-2* restored growth to wild-type levels, even though this mutant also had a large excess of γ-EC. This suggests that *jah2* is hypersensitive not only to exogenous jasmonate, but also to endogenous jasmonate, which was not elevated in the mutant. The phenotypes in soil were not likely due to enhanced pathogen sensitivity, as we saw no symptoms in pathogen-susceptible *pad2-1* or *dde2-2*, and again, the phenotype in *jah2 pad2-1* was less severe than in *jah2* (Glazebrook and Ausubel, 1994).

The function of jasmonate in defense responses is 2-fold: defense pathway activation and plant growth suppression. Repeated wounding of Arabidopsis leaves raises endogenous jasmonates and reduces leaf and plant size by a jasmonate-dependent mechanism (Yan et al., 2007; Zhang and Turner, 2008). The JAZ10/Jasmonate associated1 and COI1 coreceptors are involved, and COI1 activity requires a reducing environment and may be redox regulated in plants (Acosta and Farmer, 2010). The downstream mechanism for jasmonate-mediated growth inhibition is not entirely clear, but interaction between JAZ proteins and DELLA inhibitors of the

GA-mediated growth regulation pathway is involved (Yang et al., 2012). It is possible that excess γ-EC hyperactivates this growth repression pathway in *jah2*, even though it does not appear to involve a generalized hyperactivation of *JAZ10* or several other jasmonate-responsive genes nor an elevation of endogenous jasmonates. Our results, together with previous evidence that GSH regulates jasmonate-responsive genes, suggests that excess γ-EC is acting in a different way to affect growth than GSH does to modulate gene expression (Han et al., 2013). Allocation of resources to the competing ends of plant growth and stress response must be coordinated, and cross communication between the ascorbate-GSH cycle and jasmonate signaling appears to have an important role in optimizing this balance (Foyer and Noctor, 2011; Huot et al., 2014).

Mutants with reduced sensitivity to jasmonate have been vital to identifying jasmonate-signaling components, but few hypersensitive mutants have been described. Previously, *jah1* was shown to be hypersensitive in root inhibition, although less so than *jah2*. Induction of *PDF1.2* and *THI2.1* by MeJA was weaker in *jah1* than in the wild type (Liu et al., 2010). We also saw a reduced response for *PDF1.2* in *jah2*. We are currently examining *jah2* for pathogen and herbivore susceptibility, as well as developing a complete gene expression profile, to further explore the relationships between jasmonate and redox signaling.

In summary, we established that γ-EC is necessarily kept at much lower levels than GSH in Arabidopsis to avoid jasmonate-mediated growth suppression. The *jah2* mutant, having only a minor reduction in GSH and γ-EC levels that are only 4.5 times higher than the normal amount of GSH, offers a tool to further aid our understanding of the activity of γ-EC in plants and the close connection between jasmonate signaling and redox biology.

MATERIALS AND METHODS

Plant Material and Growth Conditions

All Arabidopsis (*Arabidopsis thaliana*) plants were of the Col-0 ecotype. The *jah2* mutant originated from a population of ethyl methanesulfonate-mutagenized M2 seeds purchased from Lehle Seeds. This mutant was recessive, based on analysis of F1 and F2 generations from a cross to the wild type (data not shown), and all experiments were done using *jah2* seed obtained after three backcrosses to Col-0. The CAPS marker primers used to identify the *jah2* allele were JAH2LP-GGGGATCAGATTGGCATAGAC and JAH2RP-GAAATAAACCACTGCGACTGC and cut with *Ssp*I. All other mutants were obtained from the Arabidopsis Biological Resource Center. Primers for genotyping *pad2-1* were PAD2LP-TCAGGAAGTTTCGTGCTGG and PAD2RP-AAACCAACCAATGTAATGTAATTG and cut with *Dde*I. Homozygous *dde2* plants were identified as male steriles and rescued by MeJA treatment. The *coi1* mutant was a male sterile transfer DNA insertion from the Salk collection (035548). PCR primers for genotyping this mutation were Coi1035548LP-TGGACCATATAAATTCATGCAGTC, Coi1035548RP-CTGCAGTGTGTAACGATGCTC, and Lba1-TGGTTCACGTAGTGGGCCATCG.

Seedling growth on Murashige and Skoog agar medium was as previously described (Staswick and Tiryaki, 2004) in an incubator at 22°C, 12-h day/night cycles, and 150 to 200 μmol s^{-1} m^{-2}. Supplementation with hormones or other compounds are as indicated in the figures. Seedling growth in sterile liquid culture was under similar conditions in 40-mL one-half-strength Murashige and Skoog medium under continuous agitation in 125-mL flasks. Plants grown in soil were in a Percival growth chamber at 22°C and 12-h day/night cycles unless otherwise noted, with fluorescent lighting at 150 to 200 μmol s^{-1} m^{-2}. Nutrients were supplied weekly using Miracle Grow complete fertilizer in water, as recommended. Tissue for thiol determination was from rosettes of soil-grown plants (5 weeks old, not bolting) frozen in liquid nitrogen and then ground to a fine powder. All experiments measuring growth were done at least three times independently, with similar results.

Synthesis of Stable Isotope γ-EC and GSH

γ-EC was synthesized from *N*-Boc-L-Glu 1-*tert*-butyl ester (Alfa Aesar) and $^{13}C_3{}^{15}N_1$-L-Cys (99% [w/w]; Cambridge Isotope Laboratories) by a mixed anhydride condensation reaction previously used for hormone-amino acid conjugate synthesis (Staswick and Tiryaki, 2004). The sulfhydryl of Cys was first reversibly protected by reaction with *S*-methyl methanethiosulfonate (Sigma-Aldrich; Smith et al., 1975). Products were fractionated by silica gel chromatography (Staswick and Tiryaki, 2004). Deprotection was accomplished in 1 mL of water in a glass tube placed in a heating block set at 110°C for 30 min (Wang et al., 2009). Reduction of the sulfhydryl was with an excess of dithiothreitol (DTT), and product was then desalted on a LH20 Sephadex column (0.5 × 30 cm) run in 75% (v/v) methanol (MeOH). Reaction products were monitored by silica thin-layer chromatography and staining with ninhydrin reagent. GSH was synthesized from fully protected γ-EC and Gly *tert*-butyl ester (Alfa Aesar) with dicyclohexylcarbodiimide (Sigma-Aldrich) as described (Cohen, 1981).

Thiol Quantification

Extraction and derivatization methods for determining γ-EC and GSH by GC/MS were developed from protocols by Roessner et al. (2006) and Humbert et al. (2001). Up to 60 mg of frozen powdered tissue was added to 400 μL of MeOH containing stable isotope internal standards added at roughly the amount recovered for the respective endogenous compounds. The mixture was homogenized 30 s with a probe homogenizer and then incubated at 70°C for 15 min, followed by addition of 400 μL of 0.2 M $NaPO_4$ (pH 6.5). Chloroform (350 μL) was added, and the mixture was vortexed, followed by brief centrifugation. The aqueous/MeOH layer (600 μL) containing polar molecules was transferred to a 1.5-mL microfuge tube with a screw cap lid. Ten microliters of freshly prepared DTT (15 mg/0.25 mL $NaPO_4$ buffer, pH 6.5) was added, mixed, and incubated 20 min at room temperature. Derivatization of SH and NH_2 groups was done by adding 100 μL of ethylchloroformate (Sigma-Aldrich) and mixing continuously on a vortex mixer as the two phases are not miscible. After 10 min, acidic residues were protonated by adding 15 μL of concentrated HCl, and then 600 μL of ethyl acetate was added, the mixture was vortexed and centrifuged, and the top ethyl acetate layer was transferred to a small glass tube for solvent evaporation under nitrogen in a 45°C water bath. The residue was dissolved in 100 μL of MeOH, and carboxyl groups were derivatized by slowly adding up to 50 μL of trimethylsilyldiazomethane (Sigma-Aldrich). Solvents were again evaporated at 45°C, and the residue was dissolved in 120 μL of ethyl acetate and transferred to a glass microvial for GC/MS.

The fraction of oxidized thiols was determined by dividing equal portions of the water/MeOH phase from the chloroform extraction into two tubes, reacting one with 15 μL of 2-vinylpyridine in the dark for 1 h, drying under N_2, and then restoring it to the original volume with 50% (v/v) MeOH. The paired samples were reduced with DTT, and the remaining steps were performed as outlined above, the difference between the two fractions being the amount of oxidized thiol in the original sample.

GC/MS used electron ionization in SIM mode. For γ-EC, the major fragmentation ions used were mass-to-charge ratios 349 and 353 for the endogenous and standard, respectively, and 363 and 366 for GSH and standard, respectively (the GSH fragment ion loses one isotope-labeled C). The molecular ions for each compound were used for validation. Quantitative data were obtained by isotope dilution from the integrated peak areas for each compound (Cohen et al., 1986). Instrumentation was a Finnigan Trace gas chromatograph with an Rtx 5MS column (15 m × 0.25 mm, 0.1 mm; Restek) coupled to a DSQ mass spectrometer. Carrier gas was helium, and the injector port was at 270°C. The oven start temperature was 120°C raised to 270°C over 15 min and held for 3 min. Transfer line and source temperatures were 280°C and 200°C, respectively. Retention time for γ-EC and GSH were 10.39 and 12.56 min, respectively.

Relative and absolute GSH/GSSG levels were also determined by a stable isotope labeling strategy using LC/MS. Briefly, in a 1.5-mL microcentrifuge tube, 50 mg of frozen powdered tissue along with 750 μL of MeOH/10 mM

phosphate (pH 7.0; 4:1, v/v) were combined. The tissue was further disrupted with a probe homogenizer. Samples were spun at 13,000*g* for 2 min, and the supernatant was collected in a new tube. Fifty microliters of the supernatant was combined with 75 μL of MeOH/10 mM phosphate (pH 7.0; 4:1, v/v) and 10 μL of isotopically labeled 1.0 M 2-vinylpyridine-d_7. The reaction was mixed and left in the dark at room temperature for 2 h. Following incubation, 50 μL of unlabeled 10 M 2-vinylpyridine was added to the reaction. After mixing, 10 μL of 0.5 M tris(2-carboxyethyl)phosphine and 5 μL of 1 mM $^{13}C_2{}^{15}N_1$-GSH were mixed into the reaction, and the tube was left in the dark for 2 h. After 2 h, the samples were dried under vacuum and reconstituted in 20 μL of 5% (v/v) MeOH. Mass spectra in positive mode were collected by a Bruker Solarix FT-ICR mass spectrometer. LC separation was performed on an ACE C18 column with a flow rate of 0.1 mL min^{-1} starting at 100% mobile phase A (0.1% [v/v] formic acid) for the first minute. Mobile phase B (acetonitrile, 0.1% formic acid) was then increased to 70% over 9 min, raised to 100% in 1 min, and then held at 100% for 1 min. The system was then returned to initial conditions and held for 7 min. Relative levels of GSH/GSSG were determined as the ratio of heavy/light vinylpyridine-labeled GSH, and absolute levels were determined by comparison with the light-labeled heavy GSH spike.

Enzyme Assay

GSH-S assays were done essentially as described (Arisi et al., 1997; Pasternak et al., 2008). The GSH product was quantified by GC/MS as described earlier, except that immediately following derivatization with ethylchloroformate, the reaction pH was neutralized with NaOH, and GSH was purified by DEAE Sephadex column chromatography, scaled down 4-fold from what was previously described (Staswick, 2009).

DNA Extraction and Genetic Mapping

Genomic DNA for mapping and genotyping of mutants was prepared as previously described (Staswick et al., 2002). F2 seeds from the cross of *jah2* to Landsberg *erecta* were plated on 1 μM MeJA agar medium, and 5-d-old seedlings were selected for short roots to identify JA-hypersensitive mutants. After growth in soil, leaf tissue was collected for DNA extraction. Known CAPS and simple sequence length repeat markers were identified through The Arabidopsis Information Resource portal (http://www.arabidopsis.org/portals/mutants/mapping.jsp). Additional markers were developed from published sequence polymorphisms between ecotypes. CAPS and simple sequence length repeat markers flanking the *JAH2* locus were CER444333, LP-CGTGAGGAATGATGATGAGG and RP-CTGGATCAGGCAAATCCTCT-3′, cut with *Alu*I; CER428256, LP-TCATGTTCCTGAGGTTGAGC and RP-CCTTGCCTCCACATTTATGA, cut with *Bfa*I; and CER449302, which has a 41-bp deletion on Landsberg *erecta*, LP-AAGATGCTTGATTGGTTGTGC and RP-CAAATTGAATTATGCACATCTAGG. Full details for the mapping strategy can be found in the thesis by Wei (2012).

Genome Sequencing and Bioinformatics

Whole-genome Illumina sequencing of *jah2* DNA was done by the Genomics Core Research Facility at the University of Nebraska. The analysis yielded a raw read count of 72.5 million reads, summed over two biological replicates (Supplemental Table S1). The Arabidopsis reference genome was downloaded from The Arabidopsis Information Resource (release TAIR10; Lamesch et al., 2012), and the replicates were individually mapped against it via the Bowtie1 (version 0.12.7; Langmead et al., 2009) short-read aligner. We used default settings, with the exception of a 32-base seed length (-l 32), three mismatches per seed (-n 3), a maximum sum of mismatch qualities across seed alignments of 180 (-e 180), and reporting of the best alignment only (–best –tryhard –k 1). The average alignment percentage of the two replicates is 95.2%. The resulting SAM output files were reformatted into a chromosome- and position-based sorted BAM file via the SAMtools software (version 0.1.16; Li et al., 2009). Subsequently, summary and likelihood data were collected for each locus by the SAMtools mpileup command utilizing the two replicates, with default parameters. The resulting VCF file was processed by the BCFtools view command (version 0.1.16; Li et al., 2009), followed by the vcfutils.pl script to filter out any SNP locus with a read depth of more than 100 (-D 100).

Complementation by Plant Transformation

Previously described methods for transformation of the wild-type GSH2 cDNA to jah2 were used (Staswick and Tiryaki, 2004). Gene expression was driven by the *Cauliflower mosaic virus* 35S promoter, and primers used to synthesize cDNA from RNA by reverse transcription-PCR were: GSH2cDNALP-CCTAGGATGGAATCACAGAAACCC and GSH2cDNARP-GGATCCTCAAATCAGATATATGCTGTCCAAG. These produced the truncated transcript lacking chloroplast-targeting signal information, hence the protein localizes to the cytosol (Pasternak et al., 2008). Seeds from primary transformants were screened for the selectable marker (kanamycin). Four initial transformants segregated 3:1 for KanR:KanS, suggesting a single transgene. These also segregated 3:1 for the wild-type root phenotype on MeJA. From two of these, homozygous transgenic lines (jah2:GSH4-3 and jah2:GSH16-3) were developed and used for the analysis.

Publicly Available Data Sets

The raw genome sequence files for *jah2* have been uploaded to National Center for Biotechnology Information's Sequence Read Archive under BioProject identification number PRJNA263382 and sample identifier SAMN03100019.

Supplemental Data

The following supplemental materials are available.

Supplemental Figure S1. Reduced and oxidized GSH.

Supplemental Table S1. Raw sequence read counts.

Supplemental Table S2. Primer sequences for semiquantitative RT-PCR.

ACKNOWLEDGMENTS

We thank the Arabidopsis Biological Resource Center for mutants *coi1* (Salk_035548) and *pad2-1* and Dr. Beat Keller for *dde2-2*.

Received July 7, 2015; accepted August 14, 2015; published August 17, 2015.

LITERATURE CITED

Acosta IF, Farmer EE (2010) Jasmonates. The Arabidopsis Book **8:** e0129, doi/10.1199/tab.0129

Arisi AC, Noctor G, Foyer CH, Jouanin L (1997) Modification of thiol contents in poplars (*Populus tremula* × *P. alba*) overexpressing enzymes involved in glutathione synthesis. Planta **203:** 362–372

Au KK, Pérez-Gómez J, Neto H, Müller C, Meyer AJ, Fricker MD, Moore I (2012) A perturbation in glutathione biosynthesis disrupts endoplasmic reticulum morphology and secretory membrane traffic in *Arabidopsis thaliana*. Plant J **71:** 881–894

Ball L, Accotto GP, Bechtold U, Creissen G, Funck D, Jimenez A, Kular B, Leyland N, Mejia-Carranza J, Reynolds H, et al (2004) Evidence for a direct link between glutathione biosynthesis and stress defense gene expression in *Arabidopsis*. Plant Cell **16:** 2448–2462

Brader G, Tas E, Palva ET (2001) Jasmonate-dependent induction of indole glucosinolates in Arabidopsis by culture filtrates of the nonspecific pathogen *Erwinia carotovora*. Plant Physiol **126:** 849–860

Browse J (2009) Jasmonate passes muster: a receptor and targets for the defense hormone. Annu Rev Plant Biol **60:** 183–205

Cairns NG, Pasternak M, Wachter A, Cobbett CS, Meyer AJ (2006) Maturation of Arabidopsis seeds is dependent on glutathione biosynthesis within the embryo. Plant Physiol **141:** 446–455

Cobbett CS, May MJ, Howden R, Rolls B (1998) The glutathione-deficient, cadmium-sensitive mutant, cad2-1, of *Arabidopsis thaliana* is deficient in γ-glutamylcysteine synthetase. Plant J **16:** 73–78

Cohen J (1981) Synthesis of ^{14}C-labelled indole-3-aspartic acid. J Labelled Compd **18:** 1393–1396

Cohen JD, Baldi BG, Slovin JP (1986) C_6-[benzene ring]-indole-3-acetic acid: a new internal standard for quantitative mass spectral analysis of indole-3-acetic acid in plants. Plant Physiol **80:** 14–19

Creissen G, Firmin J, Fryer M, Kular B, Leyland N, Reynolds H, Pastori G, Wellburn F, Baker N, Wellburn A, et al (1999) Elevated glutathione biosynthetic capacity in the chloroplasts of transgenic tobacco plants paradoxically causes increased oxidative stress. Plant Cell **11:** 1277–1292

Foyer CH, Noctor G (2011) Ascorbate and glutathione: the heart of the redox hub. Plant Physiol **155:** 2–18

Glazebrook J, Ausubel FM (1994) Isolation of phytoalexin-deficient mutants of *Arabidopsis thaliana* and characterization of their interactions with bacterial pathogens. Proc Natl Acad Sci USA **91:** 8955–8959

Grant CM, MacIver FH, Dawes IW (1997) Glutathione synthetase is dispensable for growth under both normal and oxidative stress conditions in the yeast *Saccharomyces cerevisiae* due to an accumulation of the dipeptide γ-glutamylcysteine. Mol Biol Cell **8:** 1699–1707

Han Y, Mhamdi A, Chaouch S, Noctor G (2013) Regulation of basal and oxidative stress-triggered jasmonic acid-related gene expression by glutathione. Plant Cell Environ **36:** 1135–1146

Hell R, Bergmann L (1990) λ-Glutamylcysteine synthetase in higher plants: catalytic properties and subcellular localization. Planta **180:** 603–612

Humbert B, Nguyen P, Obled C, Bobin C, Vaslin A, Sweeten S, Darmaun D (2001) Use of L-[^{15}N] glutamic acid and homoglutathione to determine both glutathione synthesis and concentration by gas chromatography-mass spectrometry (GC-MS). J Mass Spectrom **36:** 726–735

Huot B, Yao J, Montgomery BL, He SY (2014) Growth-defense tradeoffs in plants: a balancing act to optimize fitness. Mol Plant **7:** 1267–1287

Jobe TO, Sung DY, Akmakjian G, Pham A, Komives EA, Mendoza-Cózatl DG, Schroeder JI (2012) Feedback inhibition by thiols outranks glutathione depletion: a luciferase-based screen reveals glutathione-deficient γ-ECS and glutathione synthetase mutants impaired in cadmium-induced sulfate assimilation. Plant J **70:** 783–795

Lamesch P, Berardini TZ, Li D, Swarbreck D, Wilks C, Sasidharan R, Muller R, Dreher K, Alexander DL, Garcia-Hernandez M, et al (2012) The Arabidopsis Information Resource (TAIR): improved gene annotation and new tools. Nucleic Acids Res **40:** D1202–D1210

Langmead B, Trapnell C, Pop M, Salzberg SL (2009) Ultrafast and memory-efficient alignment of short DNA sequences to the human genome. Genome Biol **10:** R25

Lewandowska D, Simpson CG, Clark GP, Jennings NS, Barciszewska-Pacak M, Lin CF, Makalowski W, Brown JW, Jarmolowski A (2004) Determinants of plant U12-dependent intron splicing efficiency. Plant Cell **16:** 1340–1352

Li H, Handsaker B, Wysoker A, Fennell T, Ruan J, Homer N, Marth G, Abecasis G, Durbin R; 1000 Genome Project Data Processing Subgroup (2009) The Sequence Alignment/Map (SAM) format and SAMtools. Bioinformatics **25:** 2078–2079

Liedschulte V, Wachter A, Zhigang A, Rausch T (2010) Exploiting plants for glutathione (GSH) production: Uncoupling GSH synthesis from cellular controls results in unprecedented GSH accumulation. Plant Biotechnol J **8:** 807–820

Liu F, Jiang H, Ye S, Chen WP, Liang W, Xu Y, Sun B, Sun J, Wang Q, Cohen JD, et al (2010) The Arabidopsis P450 protein CYP82C2 modulates jasmonate-induced root growth inhibition, defense gene expression and indole glucosinolate biosynthesis. Cell Res **20:** 539–552

Mhamdi A, Hager J, Chaouch S, Queval G, Han Y, Taconnat L, Saindrenan P, Gouia H, Issakidis-Bourguet E, Renou JP, et al (2010) Arabidopsis GLUTATHIONE REDUCTASE1 plays a crucial role in leaf responses to intracellular hydrogen peroxide and in ensuring appropriate gene expression through both salicylic acid and jasmonic acid signaling pathways. Plant Physiol **153:** 1144–1160

Mikkelsen MD, Petersen BL, Glawischnig E, Jensen AB, Andreasson E, Halkier BA (2003) Modulation of CYP79 genes and glucosinolate profiles in Arabidopsis by defense signaling pathways. Plant Physiol **131:** 298–308

Noctor G, Queval G, Mhamdi A, Chaouch S, Foyer CH (2011) Glutathione. The Arabidopsis Book **9:** e0142,

Parisy V, Poinssot B, Owsianowski L, Buchala A, Glazebrook J, Mauch F (2007) Identification of PAD2 as a γ-glutamylcysteine synthetase highlights the importance of glutathione in disease resistance of Arabidopsis. Plant J **49:** 159–172

Pasternak M, Lim B, Wirtz M, Hell R, Cobbett CS, Meyer AJ (2008) Restricting glutathione biosynthesis to the cytosol is sufficient for normal plant development. Plant J **53:** 999–1012

Quintana-Cabrera R, Bolaños JP (2013) Glutathione and γ-glutamylcysteine in the antioxidant and survival functions of mitochondria. Biochem Soc Trans **41:** 106–110

Ristoff E, Hebert C, Njålsson R, Norgren S, Rooyackers O, Larsson A (2002) Glutathione synthetase deficiency: Is γ-glutamylcysteine accumulation a way to cope with oxidative stress in cells with insufficient levels of glutathione? J Inherit Metab Dis **25:** 577–584

Roessner U, Patterson JH, Forbes MG, Fincher GB, Langridge P, Bacic A (2006) An investigation of boron toxicity in barley using metabolomics. Plant Physiol **142:** 1087–1101

Rouhier N, Lemaire SD, Jacquot JP (2008) The role of glutathione in photosynthetic organisms: emerging functions for glutaredoxins and glutathionylation. Annu Rev Plant Biol **59:** 143–166

Sasaki-Sekimoto Y, Taki N, Obayashi T, Aono M, Matsumoto F, Sakurai N, Suzuki H, Hirai MY, Noji M, Saito K, et al (2005) Coordinated activation of metabolic pathways for antioxidants and defence compounds by jasmonates and their roles in stress tolerance in Arabidopsis. Plant J **44:** 653–668

Schlaeppi K, Bodenhausen N, Buchala A, Mauch F, Reymond P (2008) The glutathione-deficient mutant pad2-1 accumulates lower amounts of glucosinolates and is more susceptible to the insect herbivore *Spodoptera littoralis*. Plant J **55:** 774–786

Sharp PA, Burge CB (1997) Classification of introns: U2-type or U12-type. Cell **91:** 875–879

Smith DJ, Maggio ET, Kenyon GL (1975) Simple alkanethiol groups for temporary blocking of sulfhydryl groups of enzymes. Biochemistry **14:** 766–771

Staswick PE (2009) The tryptophan conjugates of jasmonic and indole-3-acetic acids are endogenous auxin inhibitors. Plant Physiol **150:** 1310–1321

Staswick PE, Tiryaki I (2004) The oxylipin signal jasmonic acid is activated by an enzyme that conjugates it to isoleucine in *Arabidopsis*. Plant Cell **16:** 2117–2127

Staswick PE, Tiryaki I, Rowe ML (2002) Jasmonate response locus JAR1 and several related *Arabidopsis* genes encode enzymes of the firefly luciferase superfamily that show activity on jasmonic, salicylic, and indole-3-acetic acids in an assay for adenylation. Plant Cell **14:** 1405–1415

Suza WP, Staswick PE (2008) The role of JAR1 in jasmonoyl-L: isoleucine production during Arabidopsis wound response. Planta **227:** 1221–1232

Vernoux T, Wilson RC, Seeley KA, Reichheld JP, Muroy S, Brown S, Maughan SC, Cobbett CS, Van Montagu M, Inzé D, et al (2000) The *ROOT MERISTEMLESS1/CADMIUM SENSITIVE2* gene defines a glutathione-dependent pathway involved in initiation and maintenance of cell division during postembryonic root development. Plant Cell **12:** 97–110

von Malek B, van der Graaff E, Schneitz K, Keller B (2002) The Arabidopsis male-sterile mutant dde2-2 is defective in the ALLENE OXIDE SYNTHASE gene encoding one of the key enzymes of the jasmonic acid biosynthesis pathway. Planta **216:** 187–192

Wang J, Liang YL, Qu J (2009) Boiling water-catalyzed neutral and selective *N*-Boc deprotection. Chem Commun (Camb) **2009:** 5144–5146

Wasternack C, Hause B (2013) Jasmonates: biosynthesis, perception, signal transduction and action in plant stress response, growth and development. An update to the 2007 review in Annals of Botany. Ann Bot (Lond) **111:** 1021–1058

Wei HH (2012) The hormonal characterization and mapping of a new jasmonate hypersensitive mutant (jah2) in *Arabidopsis thaliana*. MS thesis. University of Nebraska, Lincoln, Nebraska

Xiang C, Oliver DJ (1998) Glutathione metabolic genes coordinately respond to heavy metals and jasmonic acid in *Arabidopsis*. Plant Cell **10:** 1539–1550

Yan Y, Stolz S, Chételat A, Reymond P, Pagni M, Dubugnon L, Farmer EE (2007) A downstream mediator in the growth repression limb of the jasmonate pathway. Plant Cell **19:** 2470–2483

Yang DL, Yao J, Mei CS, Tong XH, Zeng LJ, Li Q, Xiao LT, Sun TP, Li J, Deng XW, et al (2012) Plant hormone jasmonate prioritizes defense over growth by interfering with gibberellin signaling cascade. Proc Natl Acad Sci USA **109:** E1192–E1200

Zhang Y, Turner JG (2008) Wound-induced endogenous jasmonates stunt plant growth by inhibiting mitosis. PLoS One **3:** e3699